PHYSICAL REVIEW B **92**, 081307(R) (2015)

Nanoscale inhomogeneity of the Schottky barrier and resistivity in MoS_2 multilayers

F. Giannazzo,[1,*] G. Fisichella,[1] A. Piazza,[1,2,3] S. Agnello,[3] and F. Roccaforte[1]
[1]*CNR-IMM, Strada VIII, 5, Zona Industriale, 95121 Catania, Italy*
[2]*Department of Physics and Astronomy, University of Catania, Catania, Italy*
[3]*Department of Physics and Chemistry, University of Palermo, Palermo, Italy*

(Received 12 June 2015; revised manuscript received 3 August 2015; published 25 August 2015)

Conductive atomic force microscopy (CAFM) is employed to investigate the current injection from a nanometric contact (a Pt coated tip) to the surface of MoS_2 thin films. The analysis of local current-voltage characteristics on a large array of tip positions provides high spatial resolution information on the lateral homogeneity of the tip/MoS_2 Schottky barrier Φ_B and ideality factor n, and on the local resistivity ρ_{loc} of the MoS_2 region under the tip. Here, $\Phi_B = 300 \pm 24$ meV, $n = 1.60 \pm 0.23$, and $\rho_{\mathrm{loc}} = 2.99 \pm 0.68\ \Omega\,\mathrm{cm}$ are calculated from the distributions of locally measured values. A linear correlation is found between the ρ_{loc} and Φ_B values at each tip position, indicating a similar origin of the ρ_{loc} and Φ_B inhomogeneities. These findings are compared with recent literature results on the role of sulfur vacancy clusters on the MoS_2 surface as preferential paths for current injection from metal contacts. Furthermore, their implications on the behavior of MoS_2 based transistors are discussed.

DOI: 10.1103/PhysRevB.92.081307 PACS number(s): 73.30.+y, 73.63.Rt, 72.80.Ga

Two-dimensional (2D) layered materials [1] are currently the object of significant scientific interests, due to their unique electrical, optical, mechanical, and chemical properties, which make them attractive both from a basic and from a technological standpoint. The most widely studied 2D material is graphene [2], both because of its rich physics and its excellent high carrier mobility. However, the lack of a band gap limits its application in electronics as a channel material for logic or switching field effect transistors. On the other hand, other layered materials, such as 2D transition metal dichalchogenides (TMDs), are semiconductors with sizable band gaps [3]. This property has opened the way to their application both in thin film transistors (TFTs) [4] as well as in novel device concepts based on vertical heterostructures of different 2D materials [1]. In particular, due to its high mechanical and chemical stability down to an ultimate single layer thickness, MoS_2 is currently being considered as a candidate to replace Si for next generation complementary metal-oxide semiconductor (CMOS) technology.

In spite of these great promises, several issues, including the scalable growth of MoS_2 films with a controlled thickness [5], the formation of low resistance Ohmic contacts [6], optimal gate dielectrics, surface passivation, and doping, are currently the objects of investigation to fully exploit the potentialities of this material.

In particular, source/drain contact resistances have been currently identified as limiting factors for MoS_2 transistor performance, leading to a severe underestimation of the field effect mobility and to a general degradation of the device characteristics [6]. MoS_2 thin films obtained by exfoliation from bulk molybdenite are typically unintentionally n-type doped [7]. Since methods for selective-area doping of MoS_2 are still lacking, source/drain contacts are typically deposited directly on unintentionally doped MoS_2, resulting in the formation of a Schottky barrier. Experiments have shown that the Schottky barrier height (SBH) values on MoS_2 can range from ~25 to ~300 meV, going from low work-function metals (such as Sc or Ti) to high work-function ones (such as Ni or Pt) [6]. Such a behavior has been commonly ascribed to a Fermi level pinning in the upper part of the MoS_2 band gap. However, the origin of this effect is still a matter of debate. Recent investigations by scanning tunneling microscopy/spectroscopy (STM/STS) have indicated that nanoscale defects present on the surface of MoS_2 can have a strong impact on the SBH [8].

In this Rapid Communication, we employ conductive atomic force microscopy (CAFM) to investigate the current injection from a nanoscale metal contact, i.e., the AFM tip, to the surface of MoS_2 thin films exfoliated on a SiO_2 substrate. CAFM has been extensively applied in the last years to locally investigate the conductivity of graphene [9], as well as the uniformity of the SBH at the junction between graphene and semiconductors [10,11]. On the contrary, this scanning probe method has been applied to a lesser extent to TMDs [12,13]. Here, a large set of local current-voltage (I-V) characteristics was measured by CAFM on the surface of MoS_2 multilayers. The analysis of these characteristics allows one to quantitatively evaluate not only the inhomogeneity of the metal/MoS_2 SBH, but also the lateral variation of MoS_2 resistivity.

MoS_2 samples were obtained by mechanical exfoliation of natural bulk molybdenite crystals purchased by SPI. The exfoliation technique was based on the use of a thermal release tape and thermocompression printing [14] on a SiO_2(300 nm)/Si substrate. A preliminary inspection of the exfoliated MoS_2 flakes was performed by optical microscopy (OM). Tapping mode atomic force microscopy (AFM) with a DI3100 AFM was employed for the precise determination of their thickness. Several MoS_2 multilayers, with thicknesses ranging from ~30 to ~60 nm, were investigated. Such relatively thick MoS_2 samples were chosen for this investigation since they guaranteed a better screening of the surface region (where the Schottky contact is formed) from the effect of charges typically present at the interface with the substrate. Figure 1(a) shows the AFM morphology in the edge region of one of the investigated MoS_2 flakes and the corresponding height

*filippo.giannazzo@imm.cnr.it

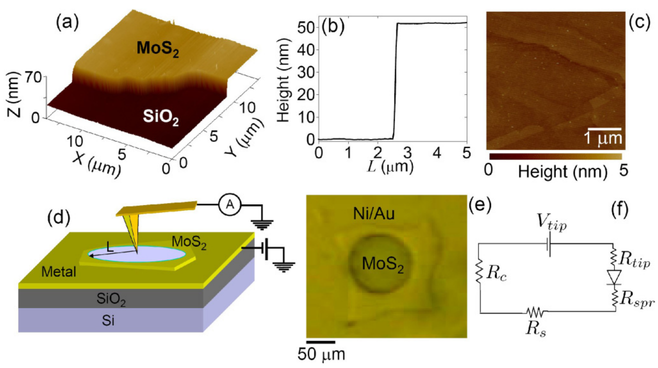

FIG. 1. (Color online) (a) AFM morphology of the edge of a multilayer MoS_2 flake and (b) corresponding height line profile, showing the thickness with respect to the SiO_2 substrate. (c) AFM image in the flake central area where CAFM measurements were performed. (d) Scheme of the experimental setup for CAFM measurements. (e) OM image of the fabricated test structure. (f) Circuital schematic representation of the measured system.

line profile [Fig. 1(b)], showing the thickness ($t \approx 50$ nm) with respect to the SiO_2 substrate. The morphology in the central area, where CAFM measurements were performed, is reported in Fig. 1(c), showing the presence of nanometer high terraces, resulting in a roughness of ~0.89 nm. Local current-voltage measurements by CAFM were performed using commercial Pt coated Si tips with a curvature radius of $r_{\mathrm{tip}} \approx 10$ nm, purchased by Nanosensors. A properly designed contact geometry consisting of a metal film with circular holes of radius $L \gg r_{\mathrm{tip}}$ [see the schematic of Fig. 1(d)] was fabricated on the MoS_2 flakes by direct writing optical lithography and the lift-off technique. The OM of a contact with radius $L \approx 50$ μm on a large MoS_2 flake is shown in Fig. 1(e). During the measurement, a bias was applied to the macroscopic contact, while the current was measured by a high sensitivity amperometer connected to the tip. Different sets of I-V characteristics were collected, displacing the tip on square arrays of tip positions in the central region of the MoS_2 flake.

A set of 25 I-V curves measured on a 500 nm × 500 nm array of tip positions with ~100 nm spacing is reported on a semilogarithmic scale in Fig. 2(a). For the sake of simplicity, the bias V_{tip} refers to the tip. Clearly, all the curves exhibit an asymmetric behavior with respect to bias inversion that can be explained as follows. The large metal contact and the nanometric tip contact to MoS_2 can be described as two Schottky diodes connected in series and in opposition. This means that when the nanometric one is forward biased (for $V_{\mathrm{tip}} > 0$), the macroscopic one is reverse biased and vice versa. However, since the nanoscale diode area is several orders of magnitude smaller (10^{-4}–10^{-6} times) than the macroscopic one, the current blocking effect of the macroscopic contact for $V_{\mathrm{tip}} > 0$ is negligible. As a result, the current transport in this system is dominated by the tip/MoS_2 local contact, and the measured I-V_{tip} characteristics resemble the forward bias behavior of this nanometric diode for $V_{\mathrm{tip}} > 0$ and the reverse bias behavior for $V_{\mathrm{tip}} < 0$.

A representative forward bias I-V_{tip} characteristic from this set of measurements is reported in Fig. 2(b). In the semilog

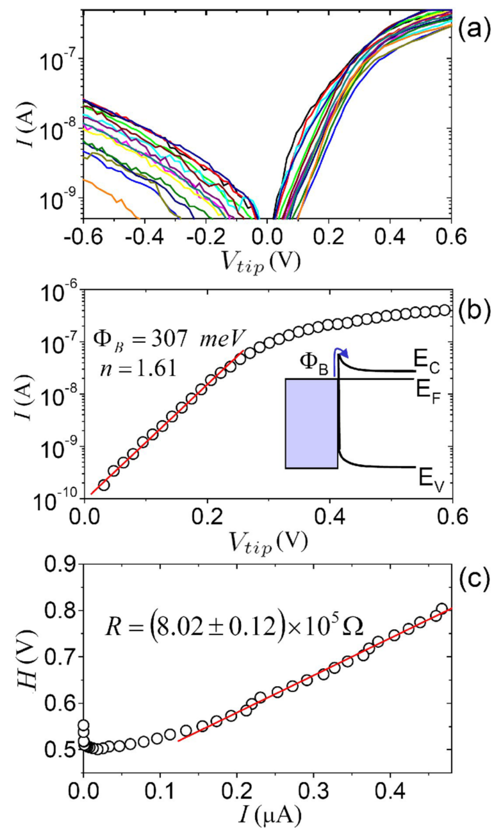

FIG. 2. (Color online) Set of 25 I-V_{tip} characteristics measured on a 500 nm × 500 nm array of tip positions with ~100 nm spacing on MoS_2. (b) Representative forward bias I-V_{tip} characteristic from this set of measurements and fit with the thermionic emission law to extract the SBH and ideality factor. Inset: Scheme of the metal/MoS_2 band structure. (c) H function plot for the determination of the series resistance R.

plot, current exhibits a more than two decades linear increase (from 1×10^{-10} to 5×10^{-8} A) with V_{tip}, followed by a saturation. A schematic representation of the band structure for this nano-Schottky diode is reported in the inset of Fig. 2(b). In order to extract the SBH Φ_B and the ideality factor n, the thermionic emission law has been applied to fit the I-V_{tip} curves in the forward bias regime,

$$I = AA^{*}T^{2}e^{-\frac{q\Phi_B}{kT}}\,e^{\frac{q(V_{\mathrm{tip}}-IR)}{nkT}}, \tag{1}$$

where q is the electron charge, k is the Boltzmann's constant, T the absolute temperature ($T = 300$ K), $A = \pi r_{\mathrm{tip}}^2$ the tip contact area, and $A^* = 4\pi q k^2 m_{\mathrm{eff}}/h^3$ the Richardson constant, with m_{eff} the effective mass for electrons in MoS_2 and h the Planck's constant. m_{eff} is slightly dependent on the MoS_2 layer number, with reported values ranging from ~$0.41m_0$ for a single layer to ~$0.57m_0$ for multilayers [15,16]. At small forward biases the weight of the resistive term R in the exponential factor of Eq. (1) is negligible and $\ln(I)$ depends linearly on V_{tip}. By linear fitting of the forward bias characteristic in the low voltage region, $\Phi_B = 307$ meV and $n = 1.61$ have been determined from the intercept and the slope of the fit, respectively. Note that, since A^* is included in a logarithmic term, its indetermination introduces only a minor error in the evaluation of the SBH. For higher bias values R causes a deviation of current from linearity and its saturation on the semilog scale. Since the downward curvature in the high voltage region of the I-$V_{\rm tip}$ curves depends both on n and R, Cheung's method [17] was applied to evaluate the R contribution. In this method, the function H is defined as $H = V_{\rm tip} - \frac{nkT}{q}\ln(\frac{I}{AA^*T^2})$, which depends on I as $H = n\Phi_B + IR$. Figure 2(c) shows a plot of H vs I obtained from the forward bias I-$V_{\rm tip}$ characteristic in Fig. 2(b). $R = (8.02 \pm 0.12) \times 10^5\ \Omega$ has been obtained by the slope of the linear fit for current values larger than 0.1 μA.

As illustrated in the circuital scheme in Fig. 1(f), R is the sum of several contributions, i.e., $R = R_{\rm tip} + R_{\rm spr} + R_s + R_c$, where $R_{\rm tip}$ is the resistance of the metal tip, $R_{\rm spr}$ is the resistance encountered by the current to spread from the nanoscale tip contact in the MoS_2 thin film, R_s is the series resistance associated to the lateral current flow from the nanoscale to the macroscopic contact, and R_c is the macroscopic contact resistance. $R_{\rm tip} \sim 1$ kΩ was preliminarily estimated by performing I-V measurements with the tip directly in contact with the metal film. For the present circular contact geometry (with perimeter $2\pi L$), $R_c \sim 0.3$ kΩ has been estimated by considering the typical specific contact resistance values ($\sim 10^5\ \Omega\,\mu$m) for Ni/Au contacts to multilayer MoS_2 [18]. $R_{\rm spr}$ and R_s are both associated with the current transport in MoS_2. However, while $R_{\rm spr}$ is related to the local resistivity $\rho_{\rm loc}$ of MoS_2 under the tip (within a hemispherical volume extending up two to three times the contact radius), R_s depends on the average resistivity of the entire MoS_2 thin film. Recently, the classical expression of the spreading resistance for a small circular contact (with radius r_c) on a semiconductor,

$$R_{\rm spr} = \frac{\rho_{\rm loc}}{4r_c}, \tag{2}$$

has been adapted also to the case of layered materials (such as graphite or MoS_2) with a strong anisotropy in the conductivity [19], replacing $\rho_{\rm loc}$ with an effective value $\rho = (\rho_\perp \rho_\parallel)^{1/2} = \gamma^{1/2}\rho_\parallel$, where $\rho_\perp$ and $\rho_\parallel$ are the out-of-plane and in-plane local resistivities, respectively, and $\gamma = \rho_\perp/\rho_\parallel$ is the anisotropy ratio. Literature results on bulk single crystalline MoS_2 samples [20] indicate that γ can range from $\sim 10^2$ to $\sim 10^4$, with typical values in the order of $\sim 10^3$. We adopted the expression of $R_{\rm spr}$ in Eq. (2), by replacing r_c with $r_{\rm tip}$.

The R_s term is mainly due to the lateral current transport within MoS_2 from the tip to the macroscopic contact and can be expressed in terms of the average value of the in-plane resistivity $\rho_\parallel$ as [10] $R_s = \frac{\rho_\parallel}{2\pi t}\ln(\frac{L}{r_{\rm tip}})$, where L is the radius of the circular hole in the metal contact and t is the MoS_2 film thickness.

Clearly, while the geometrical factors in the expressions of $R_{\rm spr}$ and R_s are in the same orders of magnitude, the local resistivity value $\rho_{\rm loc}$ is expected to be significantly higher (30–100 times) than $\rho_\parallel$ due to the high anisotropy ratio for MoS_2. As a result, $R_{\rm spr}$ is the largest resistive contribution to R. Hence, $\rho_{\rm loc}$ can be estimated from the R values measured at each tip position using Eq. (2).

By performing the same analysis on the full set of I-$V_{\rm tip}$ characteristics of Fig. 2(a), the distributions of the local SBHs, ideality factors, and resistivity values at the different tip positions on MoS_2 have been determined. The histograms of the Φ_B, n, and $\rho_{\rm loc}$ values are reported in Figs. 3(a)–3(c), respectively. It is worth mentioning that similar distributions have been obtained by analyses on several (> 10) flakes with thicknesses in the range from $\sim$30 to $\sim$60 nm, confirming that the results in Fig. 3 are representative for multilayers of MoS_2. An average SBH of 300 meV with a standard deviation of 24 meV has been estimated from the distribution in Fig. 3(a). The average Φ_B obtained by our nanoscale analysis is in good agreement with recently reported values obtained by a temperature dependent electrical characterization of MoS_2 field effect transistors with macroscopic Pt contacts [6]. Clearly, these SBH values are much lower than the ideal one expected according to the Schottky-Mott theory $\Phi_B = W_{\rm Pt} - \chi_{\rm MoS_2} \approx 1.3$ eV (with $W_{\rm Pt}$ the Pt work function and $\chi_{\rm MoS_2}$ the MoS_2 electron affinity), consistently with the commonly reported Fermi level pinning for most of the metals in the upper part of the MoS_2 band gap. The histogram in Fig. 3(b) shows that n is close to unity only on $\sim$10% of the investigated MoS_2 area, whereas the average values of n is 1.60 with a standard deviation of 0.23. Generally, the deviation of n from unity indicates that current transport is not perfectly described by the thermionic emission theory. For a macroscopic Schottky contact, this can be ascribed to several reasons, including the presence of inhomogeneities within the contact area [21] and/or to interface states [22]. In the case of a nanometric size tip-semiconductor Schottky diode, the SBH can be considered homogeneous within the contact area, whereas surface states can be responsible of $n > 1$. According to the theory of Schottky barriers with interface states [22], n can be related to the density of surface states, whereas Φ_B to their energy within the gap. The observed spread in the local Φ_B and n values indicates a spatial distribution both of

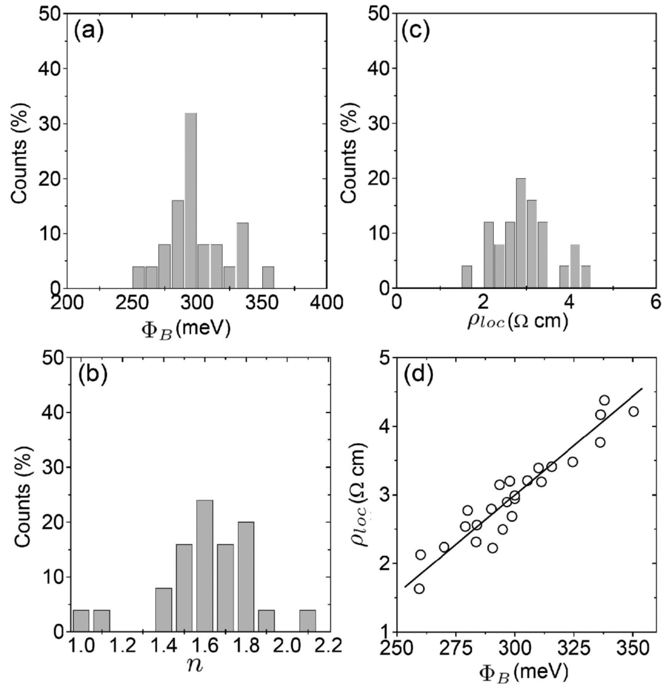

FIG. 3. Histograms of (a) the local SBH Φ_B, (b) ideality factors n, and (c) resistivities $\rho_{\rm loc}$ extracted from the full set of I-$V_{\rm tip}$ characteristics of Fig. 2(a). (d) Plot of $\rho_{\rm loc}$ vs Φ_B.

the energy and the density of the interface states. This aspect must be taken into account when the current injection from a macroscopic contact to MoS_2 is considered.

Lateral inhomogeneous Schottky barriers have been reported also for Si and compound semiconductors, and can depend on local structural/chemical inhomogeneities of the metal/semiconductor interface as well as on the presence of defects in the semiconductor surface region [21].

Finally, an average resistivity of 2.99 Ω cm with a standard deviation of 0.68 Ω cm has been estimated from the distribution in Fig. 3(c). The lateral variations of ρ_{loc} can be ascribed to inhomogeneities in the carrier concentration and/or in the carrier mobility of MoS_2. To understand whether these inhomogeneities in the transport properties have a similar origin as the inhomogeneities in the SBH, a plot of the local ρ_{loc} and Φ_B values measured at the different tip positions is shown in Fig. 3(d). A good correlation between these two quantities can be observed, with a linear increase of ρ_{loc} vs Φ_B (the fit serves as a guide to the eye). This suggests that the source for the inhomogeneous resistivity is the same as for the inhomogeneous SBH. Recent experimental investigations by STM/STS showed the formation of energy states in the band gap of MoS_2 corresponding to the intentional removal of sulfur atoms from the surface by using the electric field of STM [23]. The presence of a high density of sulfur vacancies has been demonstrated even on as-exfoliated MoS_2 from molybdenite [8]. On the other hand, sulfur vacancies are also indicated as one of the sources of n-type doping in MoS_2 [7]. It is therefore reasonable that a local increase in the density of sulfur vacancies can lead both to a reduction of the SBH and to an increase of the carrier concentration, i.e., to a reduction of ρ_{loc}.

In conclusion, nanoscale resolution CAFM analyses allowed us to evaluate the spatial inhomogeneities of the SBH and ideality factor of contacts on MoS_2, which have been ascribed to spatial variations in the density and energy of MoS_2 surface states. In addition, these analyses also provided information on the local resistivity of MoS_2, showing a nice correlation between the decrease of resistivity and that of SBH. These findings have been compared with recent literature results, which showed the role of sulfur vacancy clusters on as-exfoliated MoS_2 surfaces as preferential paths for current injection from metal contacts. Furthermore, their implications on the behavior of MoS_2 based electronic devices have been discussed.

S. Di Franco and G. Greco from CNR-IMM are acknowledged for their help in sample preparation and device characterization, respectively, and I. P. Oliveri for the collaboration in the experiments. We thank A. La Magna and I. Deretzis from CNR-IMM for useful discussions. This work has been supported, in part, by European Union Seventh Framework Programme under Grant Agreement No. 604391 Graphene Flagship.

[1] A. K. Geim and I. V. Grigorieva, Nature (London) **499**, 419 (2013).
[2] K. S. Novoselov, A. K. Geim, S. V. Morozov, D. Jiang, Y. Zhang, S. V. Dubonos, I. V. Grigorieva, and A. A. Firsov, Science **306**, 666 (2004).
[3] Q. H. Wang, K. K.-Zadeh, A. Kis, J. N. Coleman, and M. S. Strano, Nat. Nanotechnol. **7**, 699 (2012).
[4] B. Radisavljevic, A. Radenovic, J. Brivio, V. Giacometti, and A. Kis, Nat. Nanotechnol. **6**, 147 (2011).
[5] Y. Zhan, Z. Liu, S. Najmaei, P. M. Ajayan, and J. Lou, Small **8**, 966 (2012).
[6] S. Das, H.-Y. Chen, A. V. Penumatcha, and J. Appenzeller, Nano Lett. **13**, 100 (2013).
[7] H. Qiu, T. Xu, Z. Wang, W. Ren, H. Nan, Z. Ni, Q. Chen, S. Yuan, F. Miao, F. Song, G. Long, Y. Shi, L. Sun, J. Wang, and X. Wang, Nat. Commun. **4**, 2642 (2013).
[8] S. McDonnell, R. Addou, C. Buie, R. M. Wallace, and C. L. Hinkle, ACS Nano **8**, 2880 (2014).
[9] F. Giannazzo, I. Deretzis, A. La Magna, F. Roccaforte, and R. Yakimova, Phys. Rev. B **86**, 235422 (2012).
[10] S. Sonde, F. Giannazzo, V. Raineri, R. Yakimova, J.-R. Huntzinger, A. Tiberj, and J. Camassel, Phys. Rev. B **80**, 241406(R) (2009).
[11] G. Fisichella, G. Greco, F. Roccaforte, and F. Giannazzo, Nanoscale **6**, 8671 (2014).
[12] Y. Li, C.-Y. Xu, and L. Zhen, Appl. Phys. Lett. **102**, 143110 (2013).
[13] D. Fu, J. Zhou, S. Tongay, K. Liu, W. Fan, T.-J. K. Liu, and J. Wu, Appl. Phys. Lett. **103**, 183105 (2013).
[14] G. Fisichella, S. D. Franco, F. Roccaforte, S. Ravesi, and F. Giannazzo, Appl. Phys. Lett. **104**, 233105 (2014).
[15] Y. Yoon, K. Ganapathi, and S. Salahuddin, Nano Lett. **11**, 3768 (2011).
[16] M. Tosun, D. Fu, S. B. Desai, C. Ko, J. S. Kang, D.-H. Lien, M. Najmzadeh, S. Tongay, J. Wu, and A. Javey, Sci. Rep. **5**, 10990 (2015).
[17] S. K. Cheung and N. W. Cheung, Appl. Phys. Lett. **49**, 85 (1986).
[18] S.-L. Li, K. Komatsu, S. Nakaharai, Y.-F. Lin, M. Yamamoto, X. Duan, and K. Tsukagoshi, ACS Nano **8**, 12836 (2014).
[19] E. Koren, A. W. Knoll, E. Loertscher, and U. Duerig, Appl. Phys. Lett. **105**, 123112 (2014).
[20] A. Hermann, R. Samoano, V. Hadek, and A. Rembaum, Solid State Commun. **13**, 1065 (1973).
[21] R. Tung, Appl. Phys. Rev. **1**, 011304 (2014).
[22] H. Card and E. H. Rhoderick, J. Phys. D **4**, 1589 (1971).
[23] N. Kodama, T. Hasegawa, T. Tsuruoka, C. Joachim, and M. Aono, Jpn. J. Appl. Phys. **51**, 06FF07 (2012).